Forum geografic. Studii și cercetări de geografie și protecția mediului
Volume **XIX**, Issue **1** (**June** 2020), pp. **45-59**
http://dx.doi.org/**10.5775/fg.2020.040.i**

Estimation of changes in land surface temperature using multi-temporal Landsat data of Ghaziabad District, India

Anisha SINGH[1*], Varun Narayan MISHRA[1]

[1] Centre for Climate Change and Water Research, Suresh Gyan Vihar University, Jaipur, India
* *Corresponding author*: anishasingh250@gmail.com

Received on 18-03-2020, reviewed on 07-04-2020, accepted on 28-05-2020

Abstract

The rapid growth in urban population in India is seen to create an essential for the development of more urban infrastructures. Land surface temperature (LST) is a significant factor in many areas like climate change, urban land use/land cover (LULC), heat balance studies and a key input for climate models. The main objective of this paper is to examine multi-temporal land surface temperature (LST) and Normalized Difference Vegetation Index (NDVI) changes of Gaziabad district in Uttar Pradesh, India using LANDSAT satellite data in GIS platform. To compute the changes and relationship between Land Surface Temperature (LST) and Land Use Land Cover (LULC), Landsat LST data for the months of September of year 2000, 2011 and 2018 were used in this study. The LST has been estimated with respect to Normalized Difference Vegetation Index (NDVI) values determined from the Red and Near Infrared bands. The Land Surface Emissivity (LSE) is retrieved directly from the Thermal Infrared bands. The present study focuses on ArcGIS Raster functions and Raster calculation using the LANDSAT in September, thermal Bands (10, 11 & 6). The output of this paper shows that the surface temperature was high in the barren and built up area whereas it is comparatively low in the thick vegetation and agriculture land. It is also recommended that in order to reduce the land surface temperature of urban areas, sustainable urban planning strategies that include increasing the vegetated areas and embracing other green initiatives such as urban forestry should be adopted.

Keywords: *Remote sensing, GIS, Land Surface Temperature (LST), Land Surface Emissivity (LSE), Normalized Difference Vegetation Index (NDVI).*

Rezumat. O estimare a schimbărilor de temperatură a suprafeței terenului utilizând date Landsat multi-temporale din districtul Ghaziabad, India

Creșterea rapidă a populației urbane din India creează un element esențial pentru dezvoltarea mai multor infrastructuri urbane. Temperatura suprafeței terenului (LST) este un factor semnificativ în multe domenii precum schimbările climatice, utilizarea terenurilor urbane/acoperirea terenului (LULC), studiile privind echilibrul termic și un aport cheie pentru modelele climatice. Obiectivul principal al acestei lucrări este examinarea multi-temporală a temperaturii suprafeței terenului (LST) și a modificărilor Indexului de vegetație cu diferențe normalizate (NDVI) din districtul Gaziabad din Uttar Pradesh, India, folosind datele satelitului LANDSAT în platforma GIS. Pentru a calcula schimbările și relația dintre temperatura suprafeței terenului (LST) și utilizarea/acoperirea terenului (LULC), datele Landsat LST pe pentru lunile septembrie ale anului 2000, 2011 și 2018 au fost utilizate în acest studiu. LST a fost estimat în ceea ce privește valorile Indexului de vegetație cu diferențe normalizate (NDVI), determinate din benzile infraroșii și roșii. Emisivitatea suprafeței terestre (LSE) este preluată direct din benzile infraroșu termic. Studiul de față se concentrează pe funcțiile ArcGIS Raster și calculul Raster folosind LANDSAT din septembrie, benzi termice (10, 11 și 6). Rezultatul acestei lucrări arată că temperatura suprafeței a fost ridicată în zona deschisă și construită, în timp ce este relativ scăzută în zonele cu vegetație bogată și terenuri agricole. De asemenea, se recomandă ca, pentru a reduce temperatura suprafeței terenurilor din zonele urbane, să fie adoptate strategii de planificare urbană durabilă care includ densificarea zonelor de vegetație și adoptarea altor inițiative verzi, cum ar fi silvicultura urbană.

Cuvinte-cheie: *teledetecție, SIG, Temperatura suprafeței terenului (LST), Emisivitatea suprafeței terestre (LSE), Indicele de vegetație cu diferențe normalizate (NDVI).*

Introduction

Urbanization is an extreme factor of Land Use and Land Cover Change (LULC) that occurs when the natural vegetation of an area is replaced with buildings and roads, which tend to have significantly higher air temperatures than their rural surroundings. This phenomenon is described by the term Urban Heat Island (UHI) (Oke, 1982; Gartland, 2008).

Rapid changes in the land use and land cover of a region have become a major environmental concern in recent times. This has led to unsustainable development with the reduction of green spaces in the urban area and changes in local climate and formation of urban heat islands (UHIs). The UHI result defines the observation that temperatures in any urban are often higher than in its rural area (Tomlinson et al., 2010; Schwarz et al., 2012).

The identification and characterization of UHI is typically based on Land surface temperature (LST) that varies spatially, due to the nonhomogeneity of land surface cover and other atmospheric factors (Zhibin et al., 2015). LST is a key parameter in land surface processes, not only acting as an indicator of climate change, but also due to its control of the upward terrestrial radiation, and consequently, the control of

the surface sensible and latent heat flux exchange with the atmosphere (Aires, 2001; Sun and Pinker 2003). It is a key area of urban climate research (Voog and Oke, 2003; Pu et al., 2006; Niclos et al., 2009). The relationship between the LST and urban landscape patterns is the focus of many studies of the UHI effect (Dousset and Gourmelon, 2003; Weng et.al., 2004). Obtaining surface temperatures and using them in different analyses is significant to analyse the problem related with the environment (Orhan et al. 2014). Therefore, the impacts of the changes of continuous urban features and vegetation, on the variability of the urban thermal environment in different seasons needs to be examined in order to mitigate the UHI impact and adapt effectively to climate change (Zhang et al., 2017).

The UHI effect can be attributed to many physical differences between urban and rural areas, including absorption of sunlight, increased heat storage of manmade surfaces, obstruction of re-radiation by buildings, absence of plant transpiration, differences in air circulation, and other phenomena (Oke, 1982). There are two main reasons for this elevated heating in built-up areas i.e. urban materials are often water resistant, so evapotranspiration does not take place. Furthermore, impervious surfaces absorb and retain more of the sun's heat rather than natural vegetation does (Gartland, 2008) due to the darker color. Therefore, most of the world's cities experience higher temperatures in their urban core than in the surrounding sub-urban and rural areas (Gartland, 2004; Schwarz et al., 2012).

Impermeable surface areas (ISAs) i.e. built-up area and vegetation are two majors urban LULC types. Assessing the spatial distribution of impermeable surface areas and vegetation is critical for analyzing urban landscape patterns and their impact on the thermal environment (Zhang et al., 2017). The thermal comfort of city inhabitants is directly (Harlan et al., Lafortezza et al., 2009) and indirectly (Stafoggia et al., 2008) affected by UHIs. UHIs not only influence water use and biodiversity change but also contribute to human discomfort by increasing the cause of mortality and disease (Basara et al., 2010).

Remote sensing satellite data provides valuable inputs for understanding the spatio-temporal LULC in relation to the basic physical properties in terms of the surface radiance and emissivity data (Mishra and Rai, 2016; Mishra et al., 2016; Vishwakarma et al., 2016; Singh and Rai, 2017). It is an extremely useful for understanding the spatio-temporal land cover change in relation to the basic physical properties in terms of the surface radiance and emissivity data. Since the 1970s, satellite-derived (such as Landsat Thematic Mapper-TM) surface temperature data have been utilized for regional climate analyses on different scale (Amiri et al., 2009; Chander and Groeneveld, 2009; Chander et al., 2009). Nowadays thermal remote sensing has been used over urban areas to assess the urban heat island and climatic conditions. Until now, there are many studies concerning urban heat island (UHI) on regional and global climate (Rajasekar and Weng, 2009; Li et al., 2009; Li et al., 2012; Weng, 2009; Weng et al., 2004; Quattrochi and Luvall, 1999). Many studies had been made to observe the consequence of the vegetation on the LST, which showed that there was a negative correlation between LST and urban vegetation abundance measured by Normal Difference Vegetation Index (NDVI) and the percent cover of urban vegetation (Weng et al., 2004; Chen et al., 2006; Mallik et al., 2008; Senanayake et al., 2013). To analyse the thermal condition of earth features by remote sensing data, it is essential to find the relationship between the surface temperature, surrounding topography and LULC (Weng, 2009).

In India, studies concentrating on the relationship between urban vegetation and LST using Landsat TM, ETM+ and OLI imagery are rather limited. Hence through this study, it was examined the relationship between urban vegetation and LST of Ghaziabad district, India. Specific objectives of this study were: i) to calculate LST and analyses of the temporal changes in land surface temperature from 1991 to 2018; ii) to assess urban vegetation abundance, Normalized Difference Vegetation Index (NDVI) and also to investigate the relationship between LST and NDVI.

Study area

The geography of Ghaziabad gives information about the geographical details of the city of Uttar Pradesh. It lies around 1.5 km away from the Hindon river. The main rivers that flow through the Ghaziabad district are Hindon, Ganges and Yamuna. All through the year these three rivers remain full of water. Besides these main rivers, there are several other small rivers, the most remarkable among them is the river Kali. It is basically a rain-fed river. Added to this, the district uses water from the Ganga Canal for the purpose of irrigation.

The north part of Ghaziabad is bounded by Meerut district, whereas on the southern part there are Gautambudh Nagar and Bulandshahar. On the other hand, on the south-western part of Ghaziabad lies Delhi, whereas the eastern part is limited by the Jyotibaphule Nagar. Since its boundary is quite close to Delhi, Ghaziabad serves as an important entrance path to Uttar Pradesh. Therefore, Ghaziabad is popularly known as the Gateway of Uttar Pradesh, India.

While talking about the geography of Ghaziabad, it should be mentioned that this Indian city is located in between Ganges and the Yamuna plain. Its length is approximately 72 Km and the width is 37 km. According to the 1991 report it is said that the total district area was approximately 2590.0 sq. km. The climate of Ghaziabad is similar to Delhi with summer

Forum geografic. Studii și cercetări de geografie și protecția mediului
Volume **XIX**, Issue **1** (**June 2020**), pp. **45-59**
http://dx.doi.org/**10.5775/fg.2020.040.i**

temperatures ranging between 43°C to 30°C and in winter the temperature fluctuating between 25°C to 5°C. Ghaziabad Climate provides information regarding the climatic condition of the Indian city, Ghaziabad of Uttar Pradesh. Ghaziabad experiences almost the similar type of rainfall and temperature like Delhi.

It is assumed that the dust storms of Rajasthan and snowfall in the Kumaon, Himalayas and Garhwal hills play a great role in the regular alteration of Ghaziabad's weather. Generally, in Ghaziabad, the monsoon time arrives at the end of June or at the beginning of July. The city dwellers get the opportunity to enjoy this rainy season until October.

Like other northern districts of India, Ghaziabad also experiences 3 distinct seasons of winter, summer and monsoon. However, sometimes, due to extreme snowfall in the Kumaon Hills and Himalayas, adverse weather conditions occur in the city of Ghaziabad. Visitors should try to visit Ghaziabad in between the months of October and March since the temperature is very pleasant during this time. Location of the study area is shown in Fig. 1.

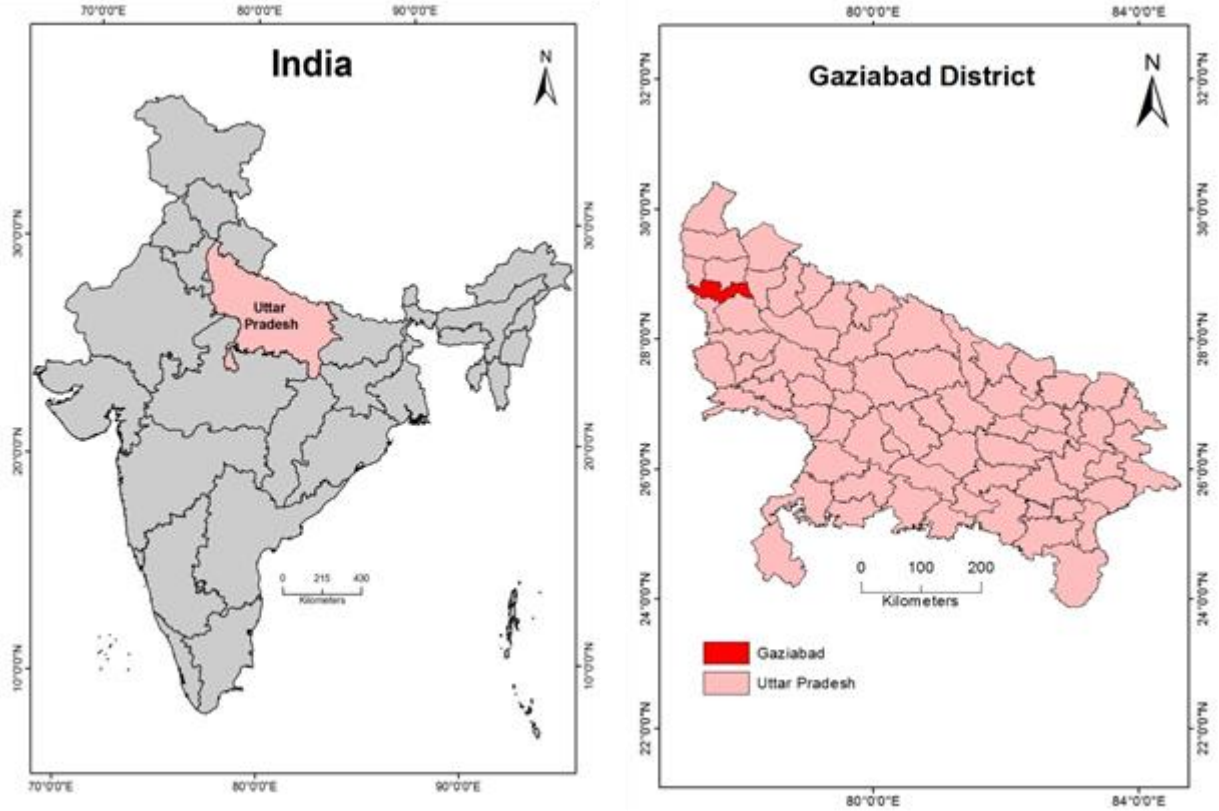

Fig 1: Location of the study area

Objective of the study

The objectives of the present study are as follows:

(a) to study the changes in LST of study area from 2000 to 2018 using Landsat satellite data;

(b) to analyse NDVI, atmosphere brightness temperature and its relationship with LST, using Landsat data.

Data used and methodology

During this study, multi-temporal Landsat data of 1992 (TM), 2000 (ETM+), 2011 (ETM+) and 2018 (OLI) are used for the analysis of temporal variation in LST in the study area. Landsat-8 carries two sensors, i.e., the Operational Land Imager (OLI) and the Thermal Infrared Sensor (TIRS). OLI collects data at a 30m spatial resolution with eight bands located in the visible and near-infrared and the shortwave infrared regions of the electromagnetic spectrum, and an additional panchromatic band of 15m spatial resolution. TIRS senses the TIR radiance at a spatial resolution of 100m using two bands located in the atmospheric window between 10 and 12μm (Juan et al., 2014; Charlie et al., 2011). Landsat-8 is the latest among the Landsat series of NRSA. The data of Landsat 8 is downloaded from the Earth Explorer website free of cost. In this study, Landsat TM of 1992, Landsat ETM+ of 2000, 2011 and Landsat-8 OLI Image of 2018 of pertaining to the study area were used to calculate NDVI and the estimation of LST. Details of Landsat data used in this study and their characteristics are given in Table 1 and Table 2.

In this study, band 10 is used to estimate brightness temperature and bands 4 and 5 are used to calculate NDVI. Two thermal bands (TIRS) capture data with a minimum of 100m resolution but are registered and delivered by the 30m OLI data product. Single-window algorithm method has been employed to find out LST

in the study area. Vegetation proportion calculation, emissivity calculation, LST calculation etc. were executed in ArcGIS-10.3 software platform. The multi-temporal Landsat satellite images were processed using ERDAS Imagine and classify the Land use/Land cover thematic map with ground truth data collected from GPS using digital image processing supervised classification method. The methodology applied in this research is illustrated in Fig. 2. Data used in this study is shown in Fig. 3 (a to d).

First, the raw data of remote sensing are used to carry out some processes. Second, the spectral indices are applied to carry out equations of LST; the land use type is extracted from Landsat. All these were used to estimate land surface temperature.

Following Meta data values are used for calculation:

- Radiance of thermal bands from Landsat 8,7,5
- K Constant bands.

Land surface temperature analysis

The most commonly LST retrieval algorithms are split window algorithm (Becker and Li, 1995; Sobrino et al., 1996), temperature/emissivity separation method, mono-window algorithm and single channel method (Jiménez-Muñoz et al., 2009). Although Landsat 8 images are provided by two thermal bands, in this study to determine LST, a single-channel algorithm was used to calculate the LST. The Landsat sensors obtain temperature data and store this information as a digital number (DN) with a range between 0 and 255. Before calculating the LST, Landsat 8 images require pre-processing to improve their quality that were done in software ENVI.

The detailed step by step process for LST calculation is given as below. Following processes have been performed for the calculation:

i. Top of Atmosphere (TOA) Radiance:

Using the radiance rescaling factor, Thermal Infra-Red Digital Numbers can be converted to TOA spectral radiance.

The following equations were adopted sequentially.

$L\lambda = ML * Qcal + AL$; (1)

Where, $L\lambda$= TOA spectral radiance (Watts/(m2*sr*μm)); (2)

ML=Radiance multiplicative band (No.)

AL= Radiance add band (No.)

Qcal= Quantized and calibrated standard product pixel values (DN).

ii. Top of Atmosphere (TOA) Brightness Temperature

Brightness temperature is the temperature of a blackbody which is used to produce the radiance perceived by the sensor, according to NASA, 2012. It is the temperature that has been received by the satellite at the time that the image was taken. Therefore, this is not the real temperature on the ground; it is the temperature at satellite (Alipour et al., 2003). TIRS band data can be converted from spectral radiance to brightness temperature using the thermal constants provided in the metadata file, the Equation 2 used to convert from spectral radiance to brightness temperature.

Spectral radiance data can be converted to top of atmosphere brightness temperature using the thermal constant Values in Meta data file.

$BT = K2 / \ln (k1 / L\lambda + 1) - 272.15$; (3)

Where, BT=Top of atmosphere brightness temperature (°C)

$L\lambda$= TOA spectral radiance (Watts/m2*sr* μm))

K1=K1 constant bans (no.)

K2=K2 constant band (no.)

iii. Normalized Difference Vegetation Index (NDVI)

NDVI is a standardized vegetation index which is calculated using Near Infra-red (Bnad 5) and Red (Band 4) bands. In this present study NDVI is used to examine the relationship between LST and greenness. The NDVI were calculated as the ratio between measured reflectance in the red and near infrared (NIR) spectral bands of the images using the following formula:

$NDVI = (NIR - RED) / (NIR + RED)$; (4)

Where, RED= DN values from the Red Band

NIR=DN values from NIR-Infrared band

The output value of NDVI ranged between -0.04 and 0.54. To get NDVI, the NDVI image was reclassified into soil and vegetation; the classified data were used to find out FVC. After generating LSE for both the bands of TIR, the mean and difference LSE was found as: $\varepsilon = (\varepsilon 10 - \varepsilon 11)/2$; (5)

$\Delta\varepsilon = \varepsilon 10 - \varepsilon 11$ (7) Where ε – Mean LSE; (6)

Δε – LSE difference; (7)

ε10 and ε11 - LSE of band 10 and 11.

Finally, the LST in kelvin was determined using SW algorithm.

iv. Land Surface Emissivity (LSE)

Land surface emissivity (LSE) is a significant parameter that describes the radiative absorption power of a surface in the long wave radiation spectrum (Tardy et al., 2016). The calculation of land surface emissivity (LSE) is required to estimate LST since LSE is a proportionality factor that scales the black body radiance (Plank's law) to measure emitted radiance and it is the ability of transmitting thermal energy across the surface into the atmosphere (Ugur and Gordana, 2016). LSE depends on the target surface top layer composition, such as presence of soil, soil type, vegetation and density, or roughness of the surface (Li et al., 2013; Sobrino et al., 2008). At the pixel scale, natural surfaces are heterogeneous in terms of variation in LSE. Land surface emissivity (LSE) is the average emissivity of an element of the surface of the Earth calculated from NDVI values.

Forum geografic. Studii și cercetări de geografie și protecția mediului
Volume **XIX**, Issue **1** (**June 2020**), pp. **45-59**
http://dx.doi.org/**10.5775/fg.2020.040.i**

PV = [(NDVI – NDVI min) / (NDVI max + NDVI min)]2; (8), where:

PV= Proportion of Vegetation

NDVI=DN values from NDVI image

NDVImin.=Minimum DN values from NDVI image

NDVImax.=Maximum DN values from NDVI image

E = 0.004 * PV + 0.986; (9) where: E=Land surface emissivity, PV=Proportion of vegetation.

v. Land Surface Temperature (LST)

LST is the radiative temperature, which is calculated using Top of atmosphere brightness temperature, Wavelength of emitted radiance, Land Surface Emissivity:

LST=(BT/1)+W*(BT/14380)*ln(E); (10)

Where, BT=Top of atmosphere brightness temperature (°C)

W=Wavelength of emitted radiance

E=Land surface emissivity

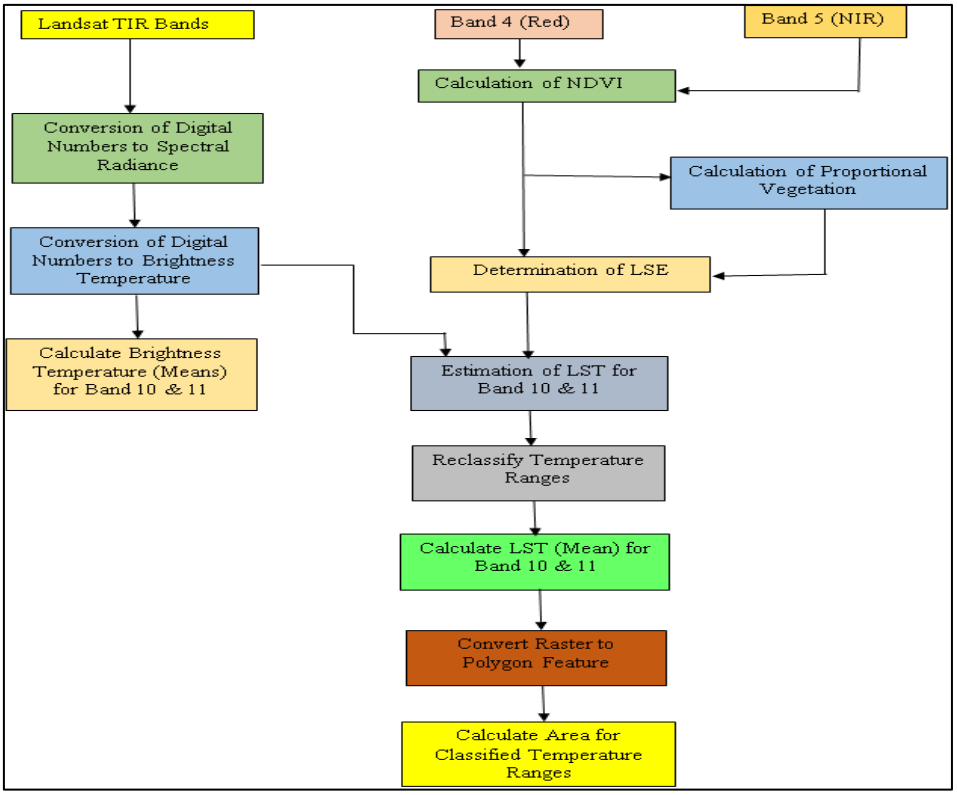

Fig. 2: Flow Chart of Methodology

Table 1 Details of Landsat Data collected for this study

Date of Acquisition	Sensor	No. of Reflective Bands	No. of Thermal Bands	Resolution (m)
September 2000	Landsat TM	06	1	30m & 120m
September 2011	Landsat ETM+	08	1	30/60
September 2018	Landsat OLI	11	1	30/60

Table 2 Characteristics of LANDSAT-8 OLI&TIRS

Bands	Wavelength (micrometers)	Resolution (meters)
Band 1 - Ultra Blue (coastal/aerosol)	0.435 - 0.451	30
Band 2 - Blue	0.452 - 0.512	30
Band 3 - Green	0.533 - 0.590	30
Band 4 - Red	0.636 - 0.673	30
Band 5 - Near Infrared (NIR)	0.851 - 0.879	30
Band 6 - Shortwave Infrared (SWIR) 1	1.566 - 1.651	30
Band 7 - Shortwave Infrared (SWIR) 2	2.107 - 2.294	30
Band 8 - Panchromatic	0.503 - 0.676	15
Band 9 - Cirrus	1.363 - 1.384	30
Band 10 - Thermal Infrared (TIRS) 1	10.60 - 11.19	30
Band 11 - Thermal Infrared (TIRS) 2	11.50 - 12.51	30

vi. Land Use Land Cover Estimation Using Supervised Classification

This study uses the maximum likelihood classification method (Liu et al., 2016; Otukei and Blaschke, 2010), in which if the observed value of a selected image sample of an unknown class is most similar to that of a sample (training) of a known class, and then it is classified as that class. According to the specific characteristics of Shenzhen land use/coverage, the land cover type is divided into the following categories: agriculture land, fallow land, barren land, vegetation, built-up area and water bodies.

Most of the studies on land coverage are based on a linear spectral mixture model, which has been successfully applied to estimate land coverage from multispectral images at the subpixel scale. The decomposition of mixed pixels based on the mixture model with three or four end members has also achieved good results in extracting land coverage. In this study, linear mixture model to calculate the components of impervious surface, vegetation, soil and shadow of each pixel of the Landsat images and compare the extracted land cover fraction with land coverage data measured on the high-resolution image are used.

The accuracy assessments provide more information on where the errors of classification happened. To know how much a classification is accurate, a set of random points must be created to evaluate the data, at the location of each random point. The result would be finding the type of land use of that spot using Google earth (truth points) and comparing it to land use of the classified raster (Jensen, 2016). Three standard criteria were used to assess the accuracy of the classifications (overall accuracy, producer's accuracy and user's accuracy).

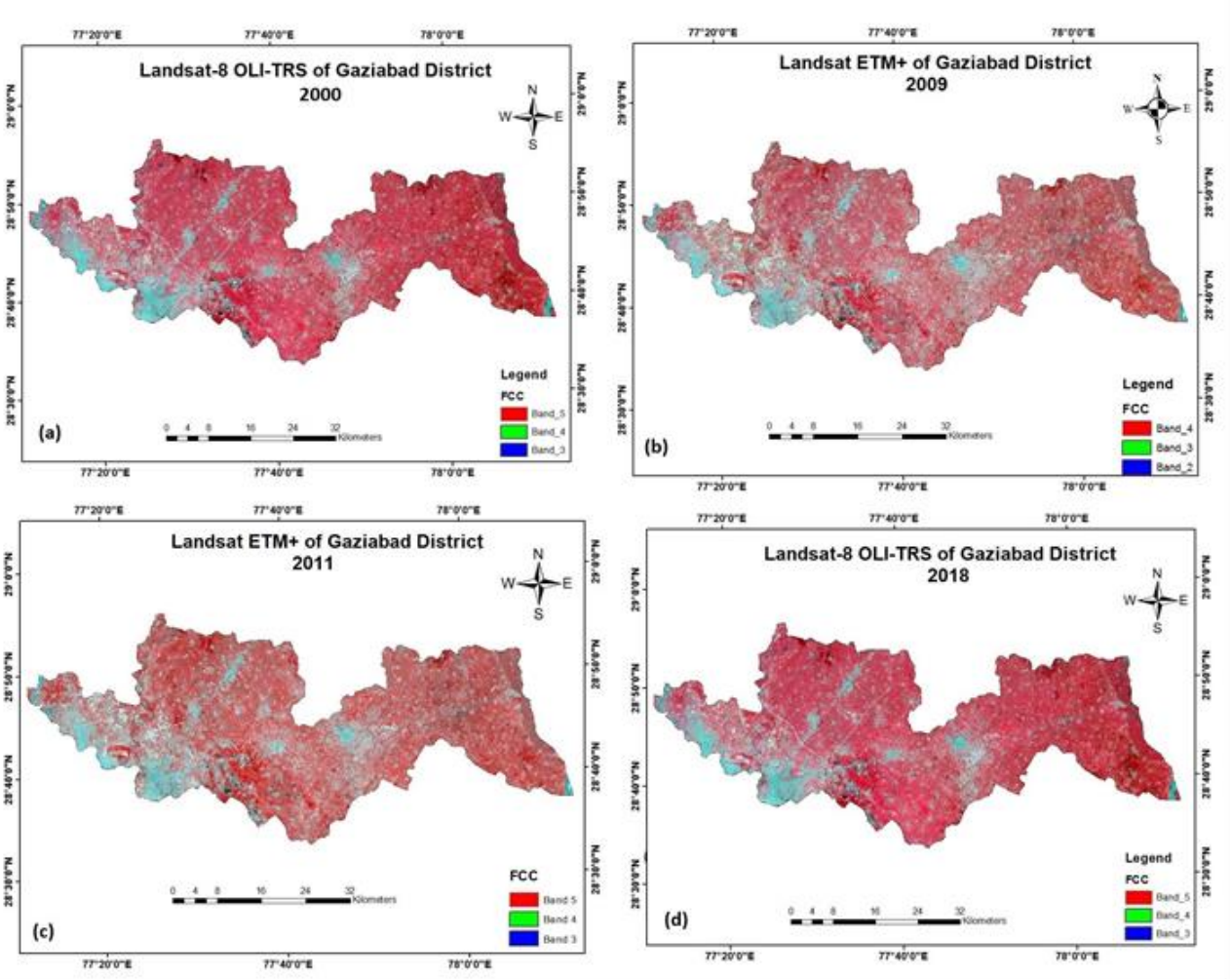

Fig. 3: False Color Composite image (FCC) of Landsat Data of 2000 (a), 2009 (b), 2011 (c) and 2018 (d) respectively.

Forum geografic. Studii și cercetări de geografie și protecția mediului
Volume **XIX**, Issue **1** (**June 2020**), pp. **45-59**
http://dx.doi.org/**10.5775/fg.2020.040.i**

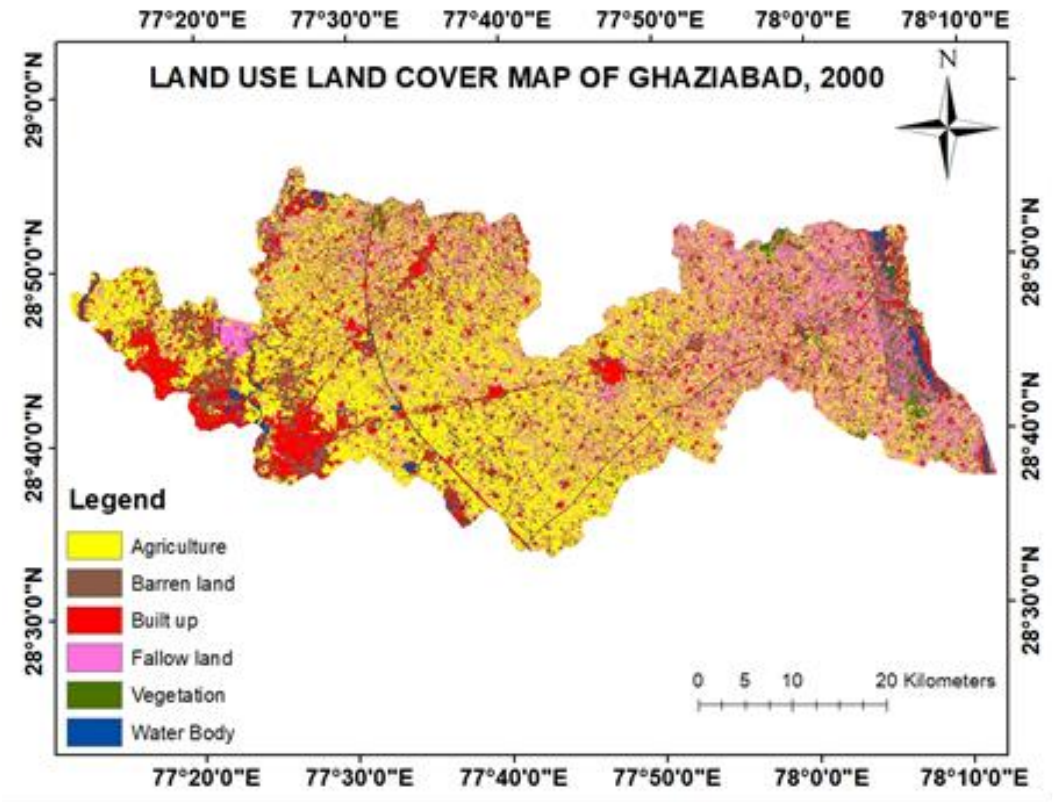

Fig. 4: Land Use Land Cover Map of Ghaziabad District in 2000

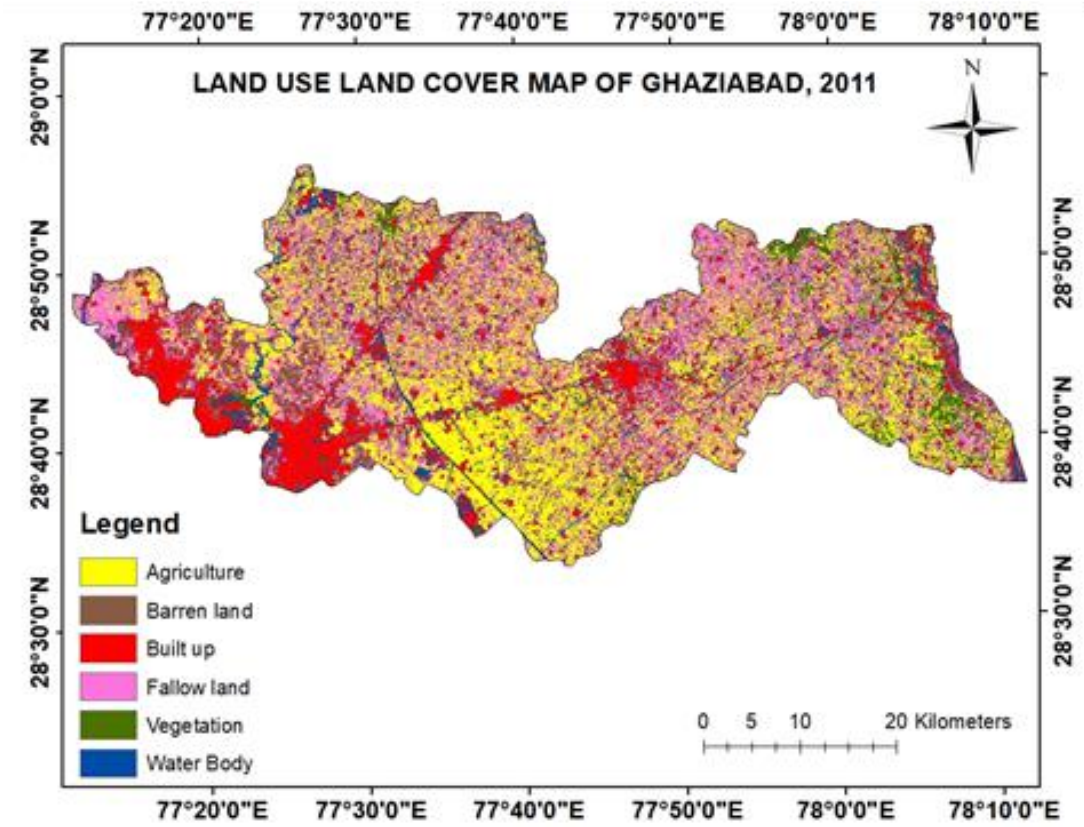

Fig. 5: Land Use Land Cover Map of Ghaziabad District in 2011

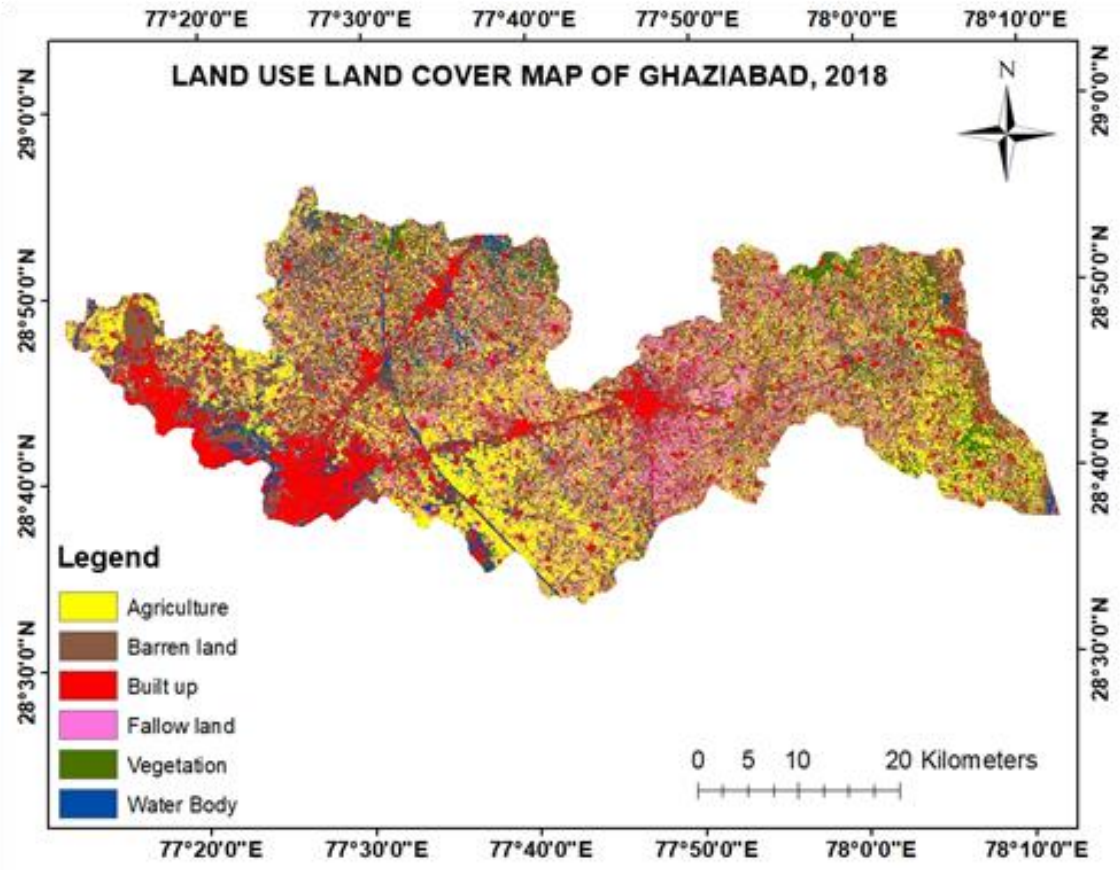

Fig. 6: Land Use Land Cover Map of Ghaziabad in 2018

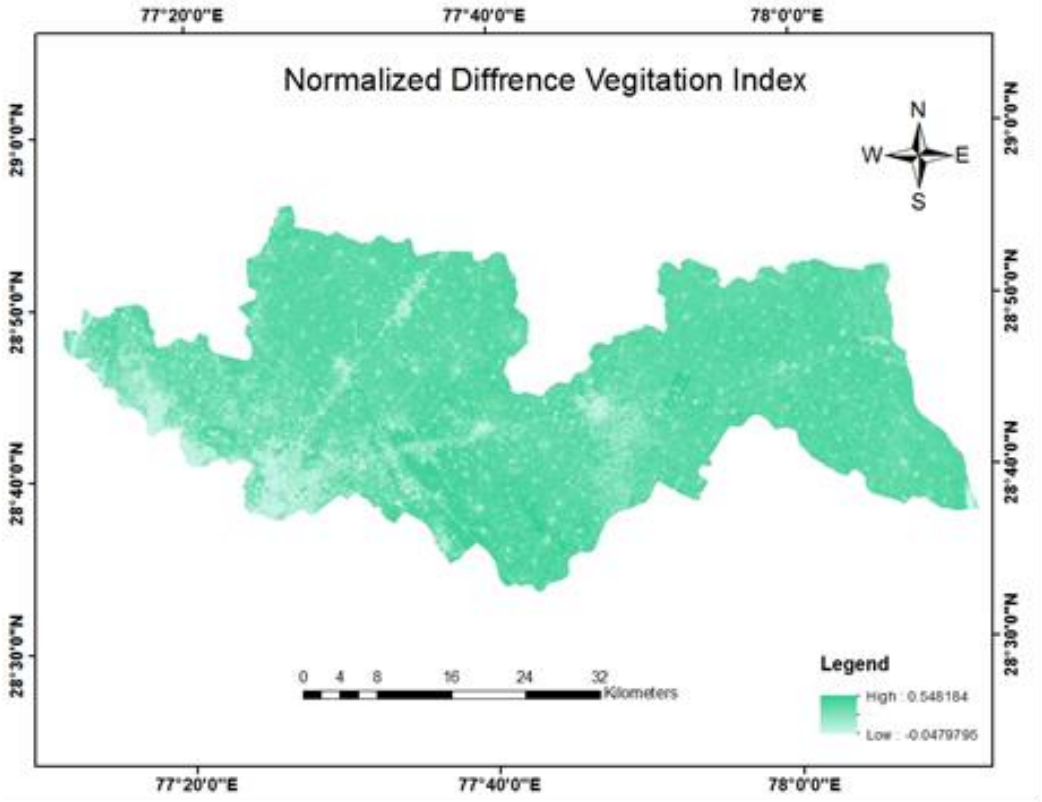

Fig. 7: Normalized Difference Vegetation Index (NDVI) in 2018

Forum geografic. Studii și cercetări de geografie și protecția mediului
Volume **XIX**, Issue **1** (**June 2020**), pp. **45-59**
http://dx.doi.org/**10.5775/fg.2020.040.i**

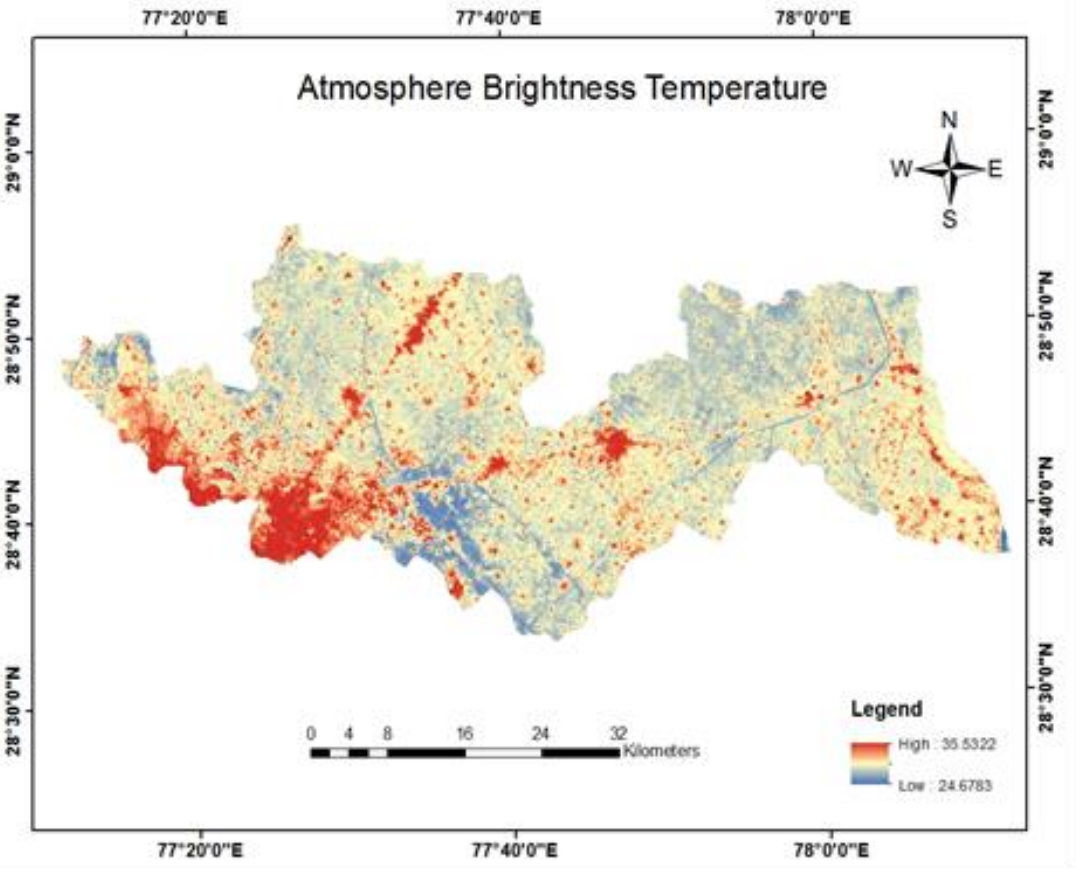

Fig. 8: Representation of Top of Atmosphere Brightness Temperature (in Degree C.) of Ghaziabad in 2018

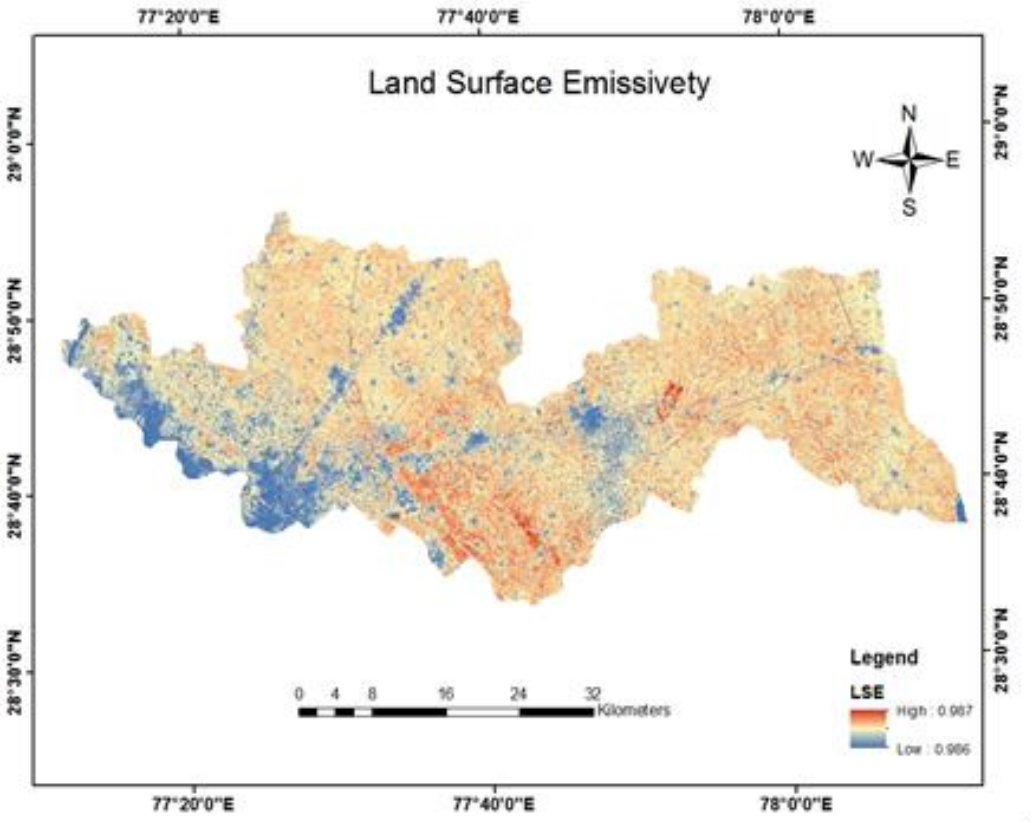

Fig. 9: Land Surface Emissivity of Ghaziabad in 2018

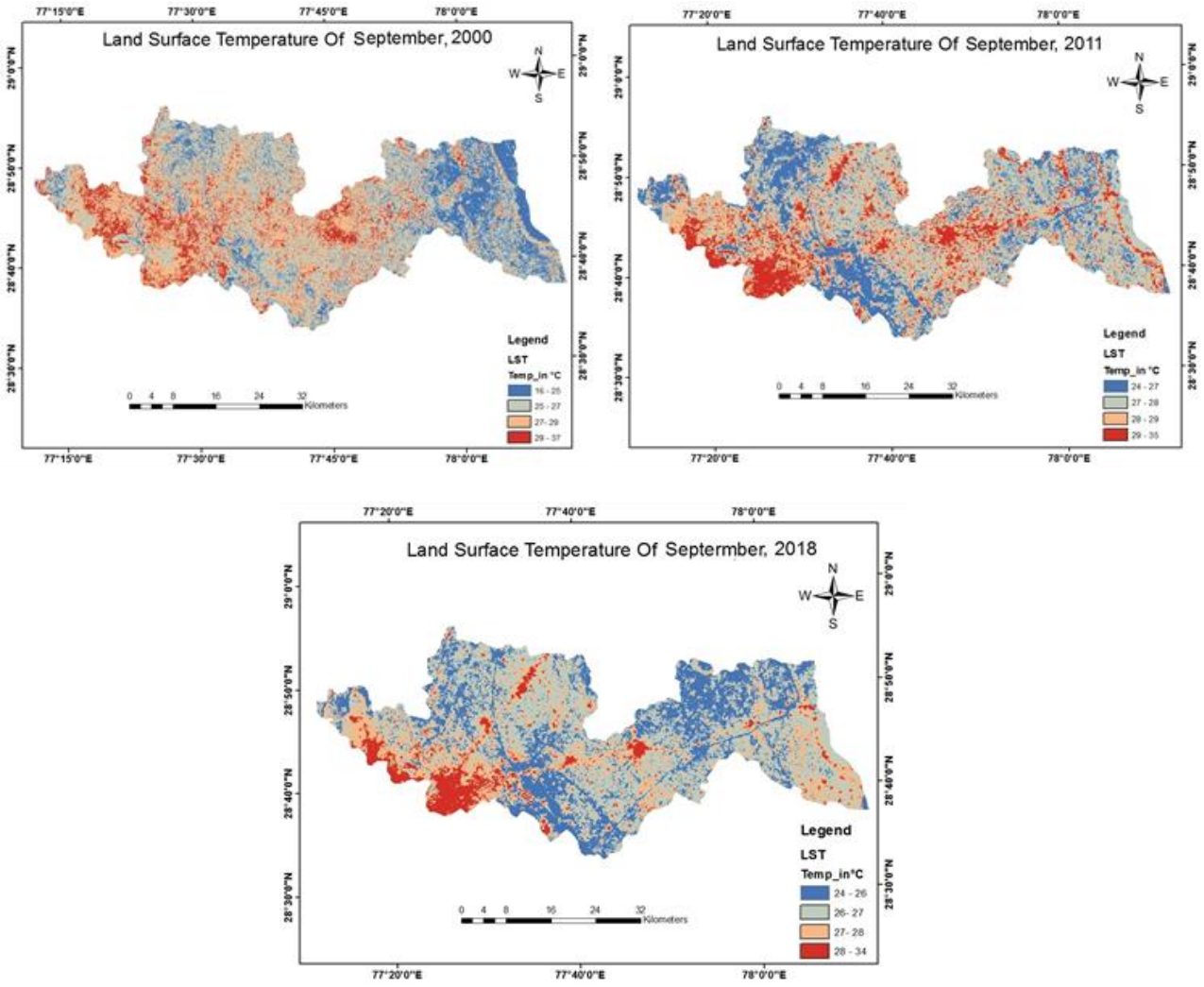

Fig. 10: Land Surface Temperature of Ghaziabad District in September 2000 (a), 2011 (b) and 2018 (c)

Table 3 Area Distribution of Each LULC classes in Ghaziabad District

LULC classes	Area (sq. km) 2000	Area (sq. km) 2011	Area (sq. km.) 2018
Agriculture	695.51	514.37	491.99
Barren land	363.40	309.27	424.00
Built up area	225.93	295.78	319.53
Fallow land	399.07	593.29	492.24
Vegetation	150.56	147.45	137.16
Water bodies	142.86	117.17	112.41
Total	1977.33	1977.33	1977.33

Results and discussion

Land Use Land Cover Change Detection

The classification of the images of the study area at different periods was necessary in the detection of changes which has occurred in the various land use within the study area over the study period. Land use changes arising from built-up area, agriculture, fallow land, barren land, vegetation and water bodies are some of the contributing factors to land cover changes in Ghaziabad district. The urban expansion witnessed in Ghaziabad is characterized by uncontrolled growth of urban development coupled with lack of appropriate land use planning and the measures for sustainable development. The changes in the LULC are described in terms of number of pixels for each classification category. Fig. 4, 5 & 6 represent LULC maps of Ghaziabad district in 2000, 2011 &

Forum geografic. Studii și cercetări de geografie și protecția mediului
Volume **XIX**, Issue **1** (**June 2020**), pp. **45-59**
http://dx.doi.org/**10.5775/fg.2020.040.i**

2018 prepared through supervised classification method. Statistics show that as in 2000, agriculture and fallow land constitutes the largest LULC categories in Ghaziabad followed by barren land and built-up area. They collectively occupy an area of 1098.58 sq km, representing 55.52% of the total land cover of the study area. The water bodies are the least land cover type. They occupied an area of 142.86 sq km which represents 7.22% of the total land cover of the study area. Observations from the 2011 show a significant increase in the built-up environment/settlement from 225.93 sq km in 2000 to 319.53 sq km in 2018, which implies an increase from 11.42% to 16.15%. Whereas, the surface covered by vegetation land decreases from 7.61% to 6.93% while barren land increased from 18.37% to 21.44%. Table 3 shows that the classification of different types of land uses land cover and its area distribution.

Normalized Difference Vegetation Index (NDVI) and Land Surface Temperature (LST)

NDVI is a measure of the vegetation density of an area and tends to reduce the increase in the alteration of natural surfaces and replacement them with impervious surfaces. It is observed that lower NDVI corresponds to the developed settlements while high NDVI values correspond to the less developed natural surfaces as presented in Fig. 7 and Fig. 11. Year 2000 has the highest NDVI value while 2018 has the lowest, which indicates that the NDVI decreases with the urban expansion. NDVI map of 2018 revealed that the NDVI value ranged between -0.04 to 0.54. The south western part of Ghaziabad district had the highest NDVI value whereas water bodies have negative value (Fig. 7). The NDVI value of the surfaces covered by vegetation was greater than 0.17 and for built-up and barren land it was 0 to 0.17.

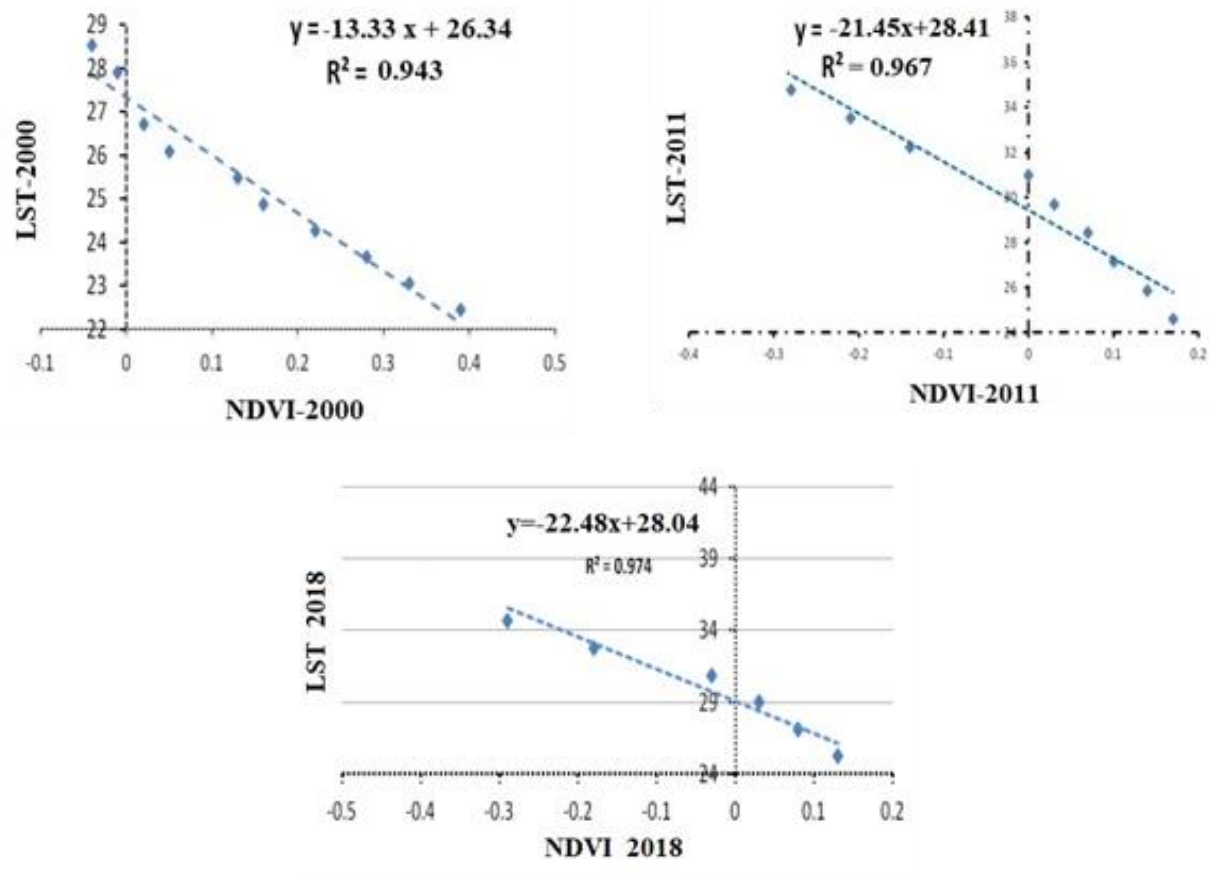

Fig. 11: Relationship between NDVI and LST for 2000, 20011 and 2018 respectively

The relationships between NDVI and LST for 2000, 2011 and 2018 respectively are shown in Fig. 11 (a to c) which show a very strong negative correlation between LST and NDVI. This figure designates that features in pixels with high NDVI values have low values and those in regions with low NDVI values have high LST. The regions with low NDVI values have less vegetation density as a result of urban growth and regions with high NDVI values have very high vegetation density. It is seen that the NDVI value decreases from 2000 to 2018 due to continuous growth in built-up area which reduced the green areas from the study area.

Land Surface Temperature (LST)

The main aim of this study was to analyse the effect of land use on LST in the urban environment. Hence, in order to evaluate the effect of different land use on LST, Landsat satellite imagery and single-channel method in ERDAS imagine and ArcGIS was used. LST was obtained in different areas of Ghaziabad in September 2000, September 2011 and September 2018 and it varied from 27.013°C and 35°C. The results of the LST estimated using the radiative transfer method presented in 2000, 2011 & 2018 are given in the table 4, 5, 6 and 7 which show that the land surface temperature in the study area increases with the increasing rate of urbanization in the city. The representation of Top of Atmosphere Brightness Temperature (in °C) and Land Surface Emissivity of Ghaziabad in 2018 is shown in Fig. 8 and 9. LST maps of Ghaziabad in 2000, 2011 and 2018 are shown in the Fig. 10 (a to c).

The table 6 and 8 show that LST over Ghaziabad has increased from a minimum of 16°C in 2000 to 24°C in 2018 which represents an increase of 8°C within 18 years resulting into an average annual increase of 0.44°C. The rapid increase in the values of LST over the years of study can be attributed to the rapid increase in the urbanization the city has witnessed. The maximum temperature reduced from 37°C to 34°C during 2000 to 2018. During 2000, 39.60% of the area was coming under 16-25°C which is the area covering under agriculture vegetation, fallow land etc.

The population of the Ghaziabad has increased from 3,290,586 in 2001 to 4,681,645 in 2011. This has led to terrible depletion of considerable number of natural surfaces and replacing them with impervious surfaces such as settlement, roads and other materials. Due to this, the capability of retaining heat increased and thereby causing serious environmental stress which in-turn, affects our urban micro-climate; but, public awareness is also increasing so that people and development authority started afforestation activity in Ghaziabad. Due to this, the maximum temperature-as seen in LST of 2018-is quite reduced.

The lowest and highest radiant temperatures for 2000 were 18.2°C (in the high-density vegetation area and agricultural land) and 30.7°C (in the built-up area) respectively. Meanwhile, for 2011, the radiant temperatures range between 24.9°C and 36.5°C; the highest temperatures were also recorded within the built-up areas while the lowest were within vegetative areas (Table 7).

Table 6 Area statistics of LST of Ghaziabad in September 2000

S. No	Temperature (°C)	Area (Sq. km)	Percentage (%)
1	16-25	782.98	39.60
2	25-27	738.33	37.34
3	27-29	352.71	17.84
4	29-37	103.30	5.22

Table 7 Area statistics of LST of Ghaziabad in September 2011

S. No	Temperature (°C)	Area (Sq. km)	Percentage (%)
1	24-27	994.73	50.31
2	27-28	542.66	27.44
3	28-29	256.34	12.96
4	29-35	183.59	9.28

Table 8 Area statistics of LST of Ghaziabad in September 2018

S. No	Temperature (°C)	Area (Sq. km)	Percentage (%)
1	24-26	993.31	50.24
2	26-27	615.67	31.14
3	27-28	216.56	10.95
4	28-34	151.78	7.68

Conclusion

This study mainly focuses on the application of using Remote Sensing data and Geographic information systems in the drive towards sustainable environmental development with interest in uneven urban development, green area loss and significant thermal changes. This study has shown the LULC dynamics of Ghaziabad at different time periods with the corresponding deviation in the thermal environment as influenced by the LULC change. In this study, LST resulting from the Landsat ETM+ and OLI spectral data proved to be a good substitute for UHI. Image-induced LST can assess urban surface temperature not only in quantity but also in spatial patterns in any highly developing city. The results shown in this study reflects that the built-up areas in Ghaziabad district has expanded significantly on the

expense of the vegetative-covered areas. The total geographical area of Ghaziabad identified in the image is equivalent to 1977.33 sq.km. In 2000, the built-up areas were 225.93 sq.km but it has increased to 319.53 sq.km. in 2018. Surface temperature variations control the surface heat and water exchange with the atmosphere resulting climatic change in the region. However, other climatic indicators play a significant role in temperature variation, the major role such as land conversion due to rapid growth of urbanization and from deforestation etc. resulting in temperature variations.

Although this study is not the end, initial outputs of this works have shown that there are noteworthy increases in the built-up areas in the Ghaziabad district which resulted in higher LST in built-up areas as compared to the vegetation areas and agricultural land. During this study, a strong negative correlation between LST and NDVI, which emphasizes that vegetation helps to reduce the LST of an area. The relationship between urban surface temperature and land cover types allowed us to find out the best solution for urban planning strategies that meet urban heat island reduction in the study area. Green space plays very important roles to improve the heat island impact by means of transpiration and heat absorption to minimize the emissivity of the hard surface reflectivity by covering the built-up area by its shadow. It is recommended to surround the highly dense built-up area and industrial areas of Ghaziabad by green belt buffers to more than 400 m for improving temperature condition and to decrease pollution effects to the acceptable limits.

References

Aires, F., Prigent, C., Rossow, W. B. & Rothstein, M. (2001). A new neural network approach including first-guess for retrieval of atmospheric water vapor, cloud liquid water path, surface temperature and emissivities over landfrom satellite microwave observations, Journal of Geophysical Research, 106, 14887-14907.

Alipour, T., Sarajian, M.R. & Esmaeily, A. (2003). Land Surface Temperature Estimation from Thermal Band of Landsat Sensor, Case Study: Alashtar City. The International Achieves of the Photogrammetry, Remote Sensing and Spatial Information Sciences, 38.

Amiri, R., Weng, Q., Alimohammadi, A. & Alavipanah S.K. (2009). Spatial–temporal dynamics of land surface temperature in relation to fractional vegetation cover and land use/cover in the Tabriz urban area, Iran. Remote Sensing of Environment, 113, 2606-2617.

Basara, J.B., Basara, H.G., Illston, B.G. & Crawford K.C. (2010). The impact of the urban heat islands during an intense heat wave in Oklahoma City. Adv. Meterol. 2010, doi:10.1155/2010/230365.

Becker, F. & Li, Z.L. (1995). Surface temperature and emissivity at various scales: Definition, measurement and related problems. Remote Sensing Reviews, 12(3-4), 225-253.

Chander, G. & Groeneveld, D.P. (2009). Intra-annual NDVI validation of the Landsat 5 TM radiometric calibration. International Journal of Remote Sensing, 30, 1621–1628.

Chander, G., Markham, B.L. & Helder, D.L. (2009). Summary of current radiometric calibration coefficients for Landsat MSS, TM, ETM+, and EO-1 ALI sensors. Remote Sensing of Environment, 113, 893–903.

Charlie, J.T., Chapman, L., John E.T. & Christopher, B. (2011). Remote Sensing Land Surface Temperature for Meteorology and Climatology: A Review, Meteorological Applications, 18: 296–306, Doi: 10.1002/met.287.

Chen, X.L., Zhao, H.M., Li, P.X. & Yin, Z.Y. (2006). Remote sensing image-based analysis of the relationship between urban heat island and land use/cover changes. Remote Sensing of Environment, 104(2), 133-146.

Cristóbal, J., Jiménez-Muñoz, J., Sobrino, J., Ninyerola, M. & Pons, X. (2009). Improvements in land surface temperature retrieval from the Landsat series thermal band using water vapor and air temperature. Journal of Geophysical Research: Atmospheres, 114(D8).

Dousset, B. & Gourmelon, F. (2003). Satellite multi-sensor data analysis of urban surface temperatures and land cover, ISPRS J. Photogrammetry Remote Sens., vol. 58, pp. 43–54.

Gartland, L. (2008). Heat Islands, Understanding and Mitigating Heat in Urban Areas; Earthscan: London, UK.

Harlan, S.L., Brazel, A.J., Prashad, L., Stefanov, W.L. & Larsen, L. (2006). Neighborhood microclimates and vulnerability to heat stress. Soc. Sci. Med. 63, 2847–2863.

Jensen, J.R., (2016). Introductory Digital Image Processing: A Remote Sensing Perspective. No. Ed. 4, Prentice-Hall Inc., Upper Saddle River.

Jiménez-Muñoz, J.C., Cristóbal, J., Sobrino, J. A., Sòria, G., Ninyerola, M. & Pons, X. (2009). Revision of the single-channel algorithm for land surface temperature retrieval from Landsat thermal infrared data. IEEE transactions on geoscience and remote sensing, 47(1), 339-349.

Jiménez-Muñoz, J. C., Sobrino, J. A., Skoković, D., Mattar, C. & Cristóbal, J. (2014). Land surface temperature retrieval methods from Landsat-8 thermal infrared sensor data. IEEE Geoscience and Remote Sensing Letters, 11(10), 1840-1843.

Lafortezza, R., Carrus, G., Sanesi, G. & Davies, C. (2009). Benefits and wellbeing perceived by

people visiting green spaces in periods of heat stress. Urban For. Urban Green, 8, 97–108.

Li, J.J., Wang, X.R., Wang, X.J., Ma, W.C. & Zhang, H. (2009). Remote sensing evaluation of urban heat island and its spatial pattern of the Shanghai metropolitan area, China. Ecological Complexity 6, 413–420.

Li, Y., Zhanga, H. & Kainz, W. (2012). Monitoring patterns of urban heat islands of the fast-growing Shanghai metropolis, China: Using time-series of Landsat TM/ETM+ data. International Journal of Applied Earth Observation and Geoinformation 19, 127–138.

Li, Z.L., Wu, H., Wang, N., Qiu, S., Sobrino, J. A., Wan, Z. & Yan, G. (2013). Land surface emissivity retrieval from satellite data. International Journal of Remote Sensing, 34(9-10), 3084-3127.

Liu, K., Su, H., Li, X. , Wang, W., Yang, L. & Liang, H. (2016). Quantifying Spatial–Temporal Pattern of Urban Heat Island in Beijing: An Improved Assessment Using Land Surface Temperature (LST) Time Series Observations From LANDSAT, MODIS, and Chinese New Satellite GaoFen-1 IEEE J. Selected Topics Appl. Earth Observat., 9, 2028-2042

Mallik, J., Yogesh K. & Bharath, B.D. (2008). Estimation of land surface temperature over Delhi using landsat-7 ETM+. J. Ind. Geophysics Union, 12(3), 131-140.

Mishra, V. and Rai, P.K. (2016). A Remote sensing Aided Multi-Layer Perceptron-Marcove Chain Analysis for Land Use and Land Cover Change Prediction in Patna district (Bihar), India, Arabian Journal of Geosciences, Vol 9 (1), 1-18, DOI: 10.1007/s12517-015-2138-.

Mishra, V.N., Rai, P.K., Kumar, P. & Prashad, R. (2016). Evaluation of Land Use/Land Covers Classification Accuracy Using Multi-Temporal Remote Sensing Images, Forum Geographic (Romania), 15 (1), 45-53.

NASA (2012). National Aeronautics and Space Administration. Goddard Earth Sciences (GES) Data and Information Services Center (DISC). https://daac.gsfc.nasa.gov/

Niclos, R., Valiente, J.A., Barbera, M.J., Estrela, M.J., Galve, J.M. & Caselles, V. (2009). Preliminary results on the retrieval of land surface temperature from MSG SEVIRI data in Eastern Spain. Proceedings pp. 55, EUMETSAT Meteorological Satellite Conference, Bath, UK, 21-25, pp. 8-19.

Oke, T. (1982). The energetic basis of the urban heat island. Quarterly Journal of the Royal Meteorological Society, 108 (455):1–24.

Orhan, O., Ekercin, S. & Dadaser-Celik, F. (2014). Use of Landsat Land Surface Temperature and Vegetation Indices for Monitoring Drought in the Salt Lake Basin Area, Turkey, The Scientific World Journal, Volume 2014, Article ID 142939, 1-11, DOI:10.1155/2014/142939.

Otukei, J.R. & Blaschke, T. (2010). Land cover change assessment using decision trees, support vector machines and maximum likelihood classification algorithms Int. J. Appl. Earth Obs. Geoinf., 12 (2010), S27-S31.

Pu, R., Gong, P., Ryo, M. & Todashi, S. (2006). Assessment of multi-resolution and multi-sensor data for urban surface temperature retrieval, Remote Sens. Environ., vol. 104, 211–225.

Quattrochi, D.A. & Luvall, J.C. (1999). Thermal infrared remote sensing for analysis of landscape ecological processes: Methods and applications. Landscape Ecology 14 (6), 577-598.

Rajasekar, U. & Weng, Q. (2009). Urban heat island monitoring and analysis using nonparametric model: a case of Indianapolis. ISPRS Journal of Remote Sensing, 64, 86–96.

Schwarz, N., Schlink, U., Franck, U. & Grossmann, K. (2012). Relationship of land surface and sir temperatures and its implications for quantifying urban heat island indicators—An application for the city of Leipzig (Germany). Ecol. Indic., 18, 693–704.

Senanayake, I., Welivitiya, W. & Nadeeka, P. (2013). Remote sensing based analysis of urban heat islands with vegetation cover in Colombo city, Sri Lanka using Landsat -7 ETM+ data. Urban Climate, 5, 19-35.

Sobrino, J., Li, Z., Stoll, M. & Becker, F. (1996). Multichannel and multi-angle algorithms for estimating sea and land surface temperature with ATSR data. International Journal of Remote Sensing, 17(11), 2089-2114.

Sobrino, J. A., Jiménez-Muñoz, J.C., Sòria, G., Romaguera, M., Guanter, L., Moreno, J. & Martínez, P. (2008). Land surface emissivity retrieval from different VNIR and TIR sensors. IEEE transactions on geoscience and remote sensing, 46(2), 316-327.

Stafoggia, M., Schwartz, J., Forastiere, F. & Perucci, C.A. (2008). Does temperature modify the association between air pollution and mortality? A multicity case-cross over analysis in Italy. Am. J. Epidemiol. 2008, 167, 1476–1485.

Sun, D. & Rachel, T.P. (2003). Estimation of land surface temperature from a Geostationary Operational Environmental Satellite (GOES-8), J. Geophys. Res.,108, 4326-4241.

Singh, S. & Rai, P.K. (2017). Application of Earth Observation Data for Estimation of Changes in Land Trajectories in Varanasi District, India, Journal of Landscape Ecology. ISSN: 1805-4196. DOI: 10.1515/jlecol-2017-0017.

Tardy, B., Rivalland, V., Huc, M., Hagolle, O., Marcq, S. & Boulet, G. (2016). A Software Tool for Atmospheric Correction and Surface Temperature Estimation of Landsat Infrared Thermal Data. Remote Sensing, 8(9), 696.

Tomlinson, C.J., Chapman, L., Thornes, J.E. & Baker, C.J. (2010). Derivation of Birmingham's summer surface urban heat island from MODIS satellite images. Int. J. Climatol., 32, 214–224.

Ugur, A. & Gordana, J. (2016). Automated Mapping of Land Surface Temperature Using LANDSAT 8 Satellite Data, Journal of Sensors, Vol. 2016, Article ID 1480307.

Voog, J.A. & Oke, T.R. (2003). Thermal remote sensing of urban climates, Remote Sens. Environ., vol. 86, 370–84.

Vishwakarma, C.S., Thakur, S., Rai, P.K., Kamal, V. & Mukharjee, S. (2016). Changing Land Trajectories: A Case Study from India Using Remote Sensing, European Journal of Geography. Vol. 7 (2), 63-73.

Weng, Q. (2009). Thermal infrared remote sensing for urban climate and environmental studies: Methods, applications, and trends, ISPRS Journal of Photogrammetry and Remote Sensing 64, 335-344.

Weng, Q., Lu, D. & Schubring, J. (2004). Estimation of land surface temperature vegetation abundance relationship for urban heat island studies. Remote sensing of Environment 89 (4): 467-483.

Zhang, Y., Balzter, H., Liu, B. & Chen, Y. (2017). Analyzing the Impacts of Urbanization and Seasonal Variation on Land Surface Temperature Based on Subpixel Fractional Covers Using Landsat Images, IEEE Journal of Selected Topics in Applied Observation and Remote Sensing, Vol. 10, No. 4, 1344-1356.

Zhibin, R., Haifeng, Z., Xingyuan, H., Dan, Z. & Xingyang, Y. (2015). Estimation of the Relationship between Urban Vegetation Configuration and Land Surface Temperature with Remote Sensing, Journal of the Indian Society of Remote Sensing, 43(1):89–100, Doi 10.1007/s12524-014-0373-9.